

Distribution and Purification of Entanglement States in Quantum Networks

Xiaojie Fan, Yukun Yang, Himanshu Gupta, C.R. Ramakrishnan

Department of Computer Science, Stony Brook University, Stony Brook, NY 11790, USA

Abstract—We consider problems of distributing high-fidelity entangled states across nodes of a quantum network. We consider a repeater-based network architecture with entanglement swapping (fusion) operations for generating long-distance entanglements, and purification operations that produce high-fidelity states from several lower-fidelity states. The contributions of this paper are two-fold: First, while there have been several works on fidelity-aware routing and incorporating purification into routing for generating EPs, this paper presents the first algorithms for optimal solutions to the high-fidelity EP distribution problem. We provide a dynamic programming algorithm for generating the optimal tree of operations to produce a high-fidelity EP, and an LP-based algorithm for generating an optimal collection of trees. Second, following the EP algorithms, this paper presents the first algorithms for the high-fidelity GHZ-state distribution problem and characterizes its optimality. We evaluate our techniques via simulations over NetSquid, a quantum network simulator.

I. Introduction

Quantum computers promise superior efficiency over classical computers for solving certain critical problems [1]. Quantum networks connecting quantum computers can enable significant applications, including quantum key distribution [2–4], communication [5], quantum sensor network [6–10] and distributed quantum computation [11–17]. These implementations fundamentally rely on the distribution of entangled states among quantum computers in the network. In this paper, we consider the efficient distribution of high-fidelity entanglement states, such as entanglement pairs (EPs) and GHZ states, by combining the purification operations with distribution strategies.

Ensuring the high fidelity of entangled states is vital for the supported applications. For instance, low fidelity of entangled pairs in quantum communication can result in errors in the teleported information [18]. Purification, where one or more entangled states are “sacrificed” to increase the fidelity of the distributed states, allows us to trade efficiency for higher fidelity. Selecting an optimal distribution strategy is crucial for reducing generation latency and guaranteeing the fidelity of entanglement states [19, 20]. Our work focuses on developing optimal distribution and purification schemes for EPs and GHZ states.

Prior Work and Our Approach. Several recent works have studied protocols for distributing entanglement states in quantum networks. Most have focused only on finding distribution strategies [21–23]. In particular, they either develop routing algorithms that do not guarantee the fidelity of the entanglement states or only consider simple purification strategies,

such as purifying only at the link level. There are fewer works on the distribution of GHZ states [24, 25], and they have restricted either the network topology or the scope of purification operations (see §IV).

In this work, we combine purification schemes with swapping/fusion trees used earlier to distribute entanglement states. We consider the problem of maximizing the rate of distributed entanglement states that are above a certain fidelity threshold. For the distribution of EPs, we develop a novel dynamic programming (DP) based algorithm that simultaneously chooses the optimal path, swapping tree, and purification scheme. We then use a linear-programming (LP) based framework, similar to those used in recent works [23, 25] on generating EPs and GHZ states, to find an optimal *collection* of purification-augmented swapping trees. We develop similar DP-based and LP-based algorithms for the distribution of GHZ states. The specifics of our algorithms are agnostic to the concrete purification model, needing only a few functions that characterize the effect of the purification operations (latency, probability of success, etc.).

Our Contributions. We formulate the problem of distributing EPs/GHZ states in quantum networks with a fidelity threshold in terms of selecting efficient purification-augmented swapping/fusion trees (see §II and §III).

- 1) We design optimal algorithms suitable for arbitrary purification models based on DP and LP for distributing EPs with fidelity above a threshold by combining the purification scheme with the swapping tree (§V).
- 2) We extend our algorithms to distributing GHZ state with fidelity above a threshold by combining the purification scheme with the fusion tree, and we propose a sub-optimal algorithm with lower time complexity (§VI).
- 3) We report the results of extensive evaluations on the NetSquid simulator, showing our solutions’ relative performance compared to prior works that use heuristic methods to combine distribution and purification (§VII).

II. Background and Models

Quantum Network (QN). A quantum network is a connected undirected graph with vertices representing quantum computers and edges representing the (quantum and classical) direct communication links. For a quantum network Q , We use *network nodes* (denoted by $V(Q)$) and *links* (denoted by $E(Q)$) to refer to its vertices and edges. Distribution of EPs and multipartite entangled states such as GHZ and graph states is generally seen as a basic *network service* based on which other

This work was partly supported by the National Science Foundation awards 2106447 and 2128187.

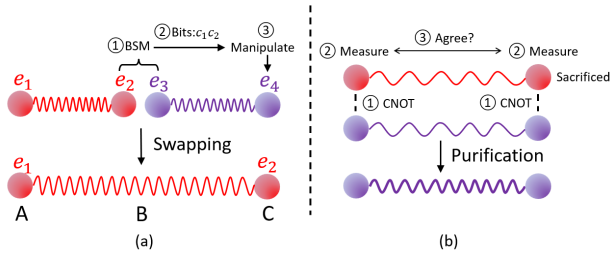


Fig. 1. (a) Entanglement swapping over the triplet of nodes (A, B, C) , which results in A 's qubit entangled with C 's qubit. (b) Purification of entanglement (blue, middle) using sacrificial EP (red, top), resulting in a higher-fidelity EP (blue, bottom) if the operation is successful.

quantum operations can be performed over the network [9, 14, 15, 26, 27]. For instance, EPs can be used to transmit arbitrary quantum data via teleportation, and implement *remote gates* (operating on qubits from different quantum computers in the network) for executing distributed quantum programs.

Model of QN. Following past work on entanglement distribution such as [23, 28], we assume each node in the network has quantum memories (possibly implemented as atomic qubits) partitioned into a collection of non-empty subsets. Each edge incident on a node is assigned a unique subset of such memories, and represents a quantum link capable of establishing an EP across the two sets of memories connected by that link. An EP established across a network link is called a “*link EP*”. The technical development of this paper is agnostic to the physical processes used to generate link EPs. We consider the link EP generation to be a Poisson process. The network model provides two functions: $rate : E(Q) \rightarrow R^+$ that gives the mean generation rate, and $fid : E(Q) \rightarrow R^+$ that gives the fidelity of link EPs. Finally, we assume that pairs of network nodes can directly communicate classical values.

Fidelity. While we attempt to share EPs/GHZ states, which are pure states, errors in their creation and distribution may result in a different, possibly mixed state. The standard definition (e.g. see [29, 30]) of the *fidelity* of a mixed state M with respect to a fixed pure state $|\psi\rangle$, denoted by $F(M)$, is $\langle \psi | M | \psi \rangle$.

A. Generation of Remote EPs

Given two link EPs shared between nodes (x_i, x_j) and (x_j, x_k) , we can create a remote EP between (x_i, x_k) by performing an *entanglement swapping* operation (ES) between the two qubits at x_j . The ES operation involves a Bell State Measurement (BSM) at x_j followed by local operation at x_i or x_k (see Fig. 1(a)). BSM is generally modeled as a *probabilistic* operation, with a success probability of p_f .

Entanglement Swapping Trees. An efficient way to generate an EP over a pair of remote network nodes (s, d) using EPs over network links (i.e., edges) is to: (i) create a path P in the network graph from s to d with EPs over each of the path's edges, and (ii) perform a series of entanglement swapping (ES) over these EPs. The ES operations over P can be performed in any order. The order can be represented by an *entanglement-swapping tree* [23]. Formally, an entanglement-swapping tree is a complete binary tree consisting of two kinds of nodes:

- leaves of the form $link(x_i, x_j)$ representing link EPs, $((x_i, x_j) \in E(Q))$ and
- internal nodes of the form $swap(x_i, x_j, x_k)$ with $x_i, x_j, x_k \in V(Q)$ representing EPs (x_i, x_j) generated by ES between (x_i, x_k) and (x_k, x_j) at network node x_k . The two children of such a node will be entanglement swapping trees, each rooted at $link(x_i, x_k)$ or $swap(x_i, x_k, -)$, and $link(x_k, x_j)$ or $swap(x_k, x_j, -)$.

Generation Latency and Generation Rate. The latency of generating EPs from an entanglement-swapping tree can be recursively computed as follows (from [23]). Let t be an entanglement-swapping tree with a *swap* node at its root. Let the two children of t be l and r . If the mean generation latencies of l and r are noted by l_l and l_r then the generation latency of t can be estimated as $l_t = L_{swap}(l_l, l_r)$ where

$$L_{swap}(l_l, l_r) = \left(\frac{3}{2} \max(l_l, l_r) + \tau_f + \tau_c\right)/p_f, \quad (1)$$

where τ_f is the latency of ES, p_f is the probability of success of ES, and τ_c is the latency of classical communication. The $\frac{3}{2}$ factor comes from the fact that given two exponential distributions with similar means $\mu_1 \approx \mu_2$ the mean of the *maximum* the two is $\approx \frac{3}{2} \max(\mu_1, \mu_2)$.

In the base case $t = link(x_i, x_j)$, latency $l_t = \frac{1}{rate(x_i, x_j)}$.

Fidelity. The fidelity of EPs generated by an entanglement-swapping tree can also be recursively computed as follows. If t has only a leaf node $link(x_i, x_j)$, then its fidelity is directly taken from that link's fidelity. Otherwise, let t have a *swap* node at its root with children l and r . Let the fidelities of EPs generated by l and r be f_l and f_r , resp. Following [31], the fidelity of EPs generated by t is $F_{swap}(f_l, f_r)$ where:

$$F_{swap}(f_l, f_r) = \frac{1}{4}(1 + \frac{1}{3}(4f_l - 1)(4f_r - 1)) \quad (2)$$

The above assumes noiseless swap operations. Noisy swap operations can be easily modeled as in [31, 32]; but since it does not change our technical development or algorithms, we only show the simpler noise-free model here.

B. Incorporating Purification into Generation Schemes

Ensuring the fidelity of EPs and GHZ states is crucial since they are used as the basis for other operations in distributed computing. *Entanglement Purification* [30] is obtaining high-fidelity EPs and GHZ states from multiple copies of lower-fidelity states.

Purification of EP. Let t (“target”) and s (“sacrificial”) be two pairs of qubits with fidelities F_t and F_s with respect to $|\Phi^+\rangle$. Purification [20, 30, 33] of t using s succeeds with a certain probability, leaving t in a higher-fidelity state. When purification fails, t is discarded. Qubits in s are discarded at the end, regardless of the operation's success.

The fidelity of t , when the operation succeeds, and the success probability are functions of the initial fidelity of t and s ; we denote these functions by $F_{pur}(F_t, F_s)$, and $p_{pur}(F_t, F_s)$,

respectively. For instance, the Bennett *et al* purification protocol [30] yields the following two definitions for the functions:

$$p_{pur}(F_t, F_s) = F_t F_s + F_t \left(\frac{1-F_s}{3}\right) + \left(\frac{1-F_t}{3}\right) F_s + 5 \left(\frac{1-F_t}{3}\right) \left(\frac{1-F_s}{3}\right) \quad (3)$$

$$F_{pur}(F_t, F_s) = \frac{F_t F_s + \left(\frac{1-F_t}{3}\right) \left(\frac{1-F_s}{3}\right)}{p_{pur}(F_t, F_s)} \quad (4)$$

It is easy to see that $F_{pur}(f_t, f_s) > f_t$ when $0.5 < f_s, f_t < 1$. The above definition of F_{pur} and p_{pur} assumes that the purification operations themselves are noiseless; incorporating noise is straightforward, already shown in [20], does not add to the technical development here, and hence is omitted. The techniques developed in this work can be easily generalized to other purification models and quantum channels.

Iterated Purification. The protocol by Deutsch *et al.* [33] omits a depolarization step and results in better yield. Both [30, 33], when used for repeated purification, assume $f_t = f_s$, thereby performing a balanced tree of purifications. The “entanglement pumping” method of [20] builds a skewed purification tree and reduces resource needs. Specifically, this method iteratively purifies t using identical copies of s . Let $F_{pur,i}$ denote the fidelity of t at the end of the i -th step. Then:

$$F_{pur,i}(f_s) = \begin{cases} f_s & i = 0 \\ F_{pur}(F_{pur,i-1}(f_s), f_s) & i > 0 \end{cases} \quad (5)$$

Let $p_{pur,i}$ denote the probability of success of the i -th step.

$$p_{pur,i}(f_s) = \begin{cases} 1 & i = 0 \\ p_{pur}(F_{pur,i-1}(f_s), f_s) & i > 0 \end{cases} \quad (6)$$

III. Problem Definition

In this section, we formally define the problems of optimal generation of EPs and GHZ states using entanglement swapping and purification operations.

A. EP Distribution with Purification

Purification-Augmented Swapping Tree. In the presence of purification operations and the goal of establishing EPs of a given fidelity, we generalize entanglement-swapping trees of §II-A to purification-augmented swapping trees. In addition to *link* and *swap* nodes, a purification-augmented swapping tree may contain (unary) nodes of the form $purify(x_i, x_j, k)$ denoting a purification operation to generate an EP (x_i, x_j) using k additional sacrificial copies. Since the purification operation expects EP (x_i, x_j) , the child of a $purify(x_i, x_j, k)$ node may be any node that produces EP (x_i, x_j) ; and a $purify(x_i, x_j, k)$ may occur wherever EP (x_i, x_j) may be an operand. See Fig. 2 is an example.

The calculation of generation latency follows from entanglement swapping trees, with the following additional definition that captures the impact of purification on latency. Let t be a tree with $purify(x_i, x_j, k)$ as its root with t' as its child. Let $l_{t'}$ be the generation latency of t' , and $f_{t'}$ be the fidelity of EPs

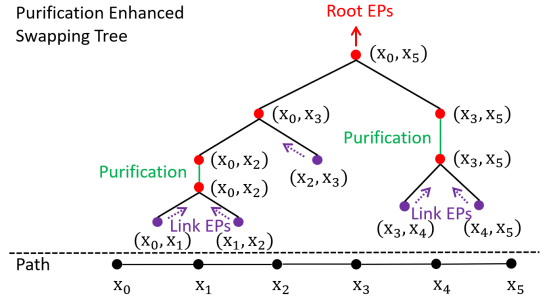


Fig. 2. A purification-augmented swapping tree over a path. Binary internal nodes perform entanglement swapping, and unary nodes do purification. The leaves of the tree generate link EPs and internal nodes generate remote EPs.

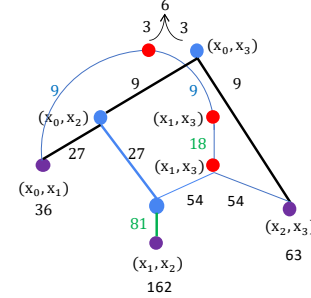


Fig. 3. Example level-based fusion structure. This “aggregates” of two purification-augmented swapping trees. For illustration, the figure assumes that a parent’s generation rate is 1/3 of the rate of its children for swapping and 1/2 for purification. The leaf node (x_0, x_1) ’s generation rate of 36 units is “split” into 9 and 27 for the two different (red and blue) swapping operations. The two root nodes represent the final/target EP formed in two different ways—for a total generation rate of 6 (3 from each swapping operation). Unary nodes represent the results of purification operations.

generated by t' . Based on iterated purification, the latency of t , $l_t = L_k(l_{t'}, f_{t'})$ where L_i is defined as:

$$L_i(l, f) = \begin{cases} l & i = 0 \\ \frac{(L_{i-1}(l) + l + \tau_p + \tau_c)}{p_{pur,i-1}(f)} & i > 1 \end{cases} \quad (7)$$

In the above, τ_p and τ_c are the latency of purification and classical communication, and $p_{pur,i}$ is defined in Eqn. 6.

EP Distribution with Purification (EDP) Problem. Given a quantum network Q , a pair of nodes (s, d) , and a required fidelity threshold f , the EDP problem is to determine a single purification-augmented swapping tree that maximizes the generation rate (i.e., minimizes the expected generation latency) of EPs (s, d) with fidelity no less than f . \square

We now generalize the EDP problem to consider concurrent swapping trees.

Level-Based Fusion Structure. To maximize the generation rate of EPs, *multiple concurrent* purification-augmented swapping trees may be required to use all available network resources. Since the number of such trees can be exponential, we use a novel “aggregated” structure that aggregates multiple (purification-augmented swapping) trees into one structure; we refer to this as a *level-based* structure, as it is composed of multiple levels—with each level consisting of EPs (as vertices) created by swapping operations and purification operations from the previous levels. See Fig. 3. The bottom level consists of link EPs and each non-leaf EP S is formed by a swapping

operation or a purification operation of pairs of EPs (or one EP) in the previous layers; however, there may be several such operations that create S (in different ways). Each EP S may also have multiple “parents” (unlike in a tree), i.e., an EP S may be used to create several EPs in the next layer; in such a case, the generation rate of S is “split” across these operations. Due to the operations from previous layers, each vertex/EP has a resulting generation rate, estimated as discussed in III.

Generalized EDP (GEDP) Problem. Given a quantum network Q , and a set $\Delta = \{(s_i, d_i), f_i\}$ of source-destination pairs, along with the fidelity threshold for each pair, the GEDP problem is to determine a level-based structure that generates EPs with fidelity above the threshold over the giving pairs of nodes with the optimal (highest) generation rate. \square

B. GHZ Distribution with Purification

GHZ states can be generated across network nodes using *fusion* operations, fusing smaller GHZ states to get a larger state. The fusion operations implicitly considered in our work are the same as those used in [25]. The fidelity of GHZ states can be increased using purification operations analogous to that used for EPs. Consequently, we can define a “*purification-augmented fusion tree*” to order the operations for generating a distributed GHZ state. Latency and fidelity can be calculated analogously as well.

The “*GHZ Distribution with Purification (GDP) Problem*” is a direct generalization of the EDP problem to GHZ states. “*Generalized GDP (GGDP) Problem*” generalizes this further to obtain a version of the GEDP problem for GHZ states.

IV. Related Works

The seminal work of Dür *et al* [31] introduced repeater-based quantum networks where entanglement swapping operations were interleaved with purification. That work considered only a path and focused on placing repeater nodes to ensure a balanced optimal tree of operations. Several network protocols that followed considered on entanglement routing without purification [21, 23, 28, 34, 35, e.g.]. Other works that include purification for distributing EPs and GHZ states are elaborated below.

Distribution of EP. A few studies have been conducted on using purification in the distribution of EP. In particular, [36] is the first to address end-to-end fidelity for remote EPs, identifying the top k shortest paths between the source and destination. For each path, they first perform purification operations to let all the link EPs above a link fidelity threshold, then iteratively purify the link most critical to end-to-end fidelity until the goal end-to-end threshold is reached, and use linear programming to allocate limited resources among different paths, maximizing the number of entanglement connections. However, compared to our work, they consider much simpler purification schemes: using purification only at link EPs. We evaluate and compare the above work with ours in §VII.

The works [37–42] consider purification only at the link-level or top-level to make the fidelity above a threshold. Prior

works [43, 44] considered performing purification for the intermediate EPs generated while doing entanglement swapping operations; however, they only discussed purification within the context of balanced swapping trees. [43] uses Dijkstra’s algorithm to find the shortest path without considering the order of swap operations. [44] proposed a Dijkstra-like algorithm that maintains a priority queue to find the shortest path in a quantum network by gradually expanding paths from the source node, prioritizing them based on the number of hops and available resources, while ensuring that entanglement fidelity requirements are met. However, their approach only considered a balanced swapping tree and two basic purification schemes: purifying at the link level and purifying to restore the original fidelity of the new entangled pairs before swapping. Finally, [45, 46] develop optimal purification “schedule” over a *given* entanglement path, restricting themselves to purification only for link-level EPs. They also develop an approximation scheme for selecting an entanglement path based on the designed purification scheme; we note that they use the “synchronized” swapping model, vastly different from our memory-assisted “waiting” model [23], which entails the selection of swapping trees rather than just swapping paths.

Distribution of GHZ states. For GHZ states, most of the existing works only generate high fidelity GHZ states at the same node [47–50]. [51, 52] explore the purification protocol space of purifying a GHZ state with another GHZ state of smaller or the same size and combine purification with the distribution of GHZ states; their solutions only work on quantum networks with specific simple topology.

V. Optimal Solutions to the EDP and GEDP Problems

In this section, we will begin by discussing the key challenges and basic idea to solving the EDP problem. Then, we will introduce a dynamic programming algorithm to find the optimal purification-augmented swapping tree.

A. Optimal DP Solution for the EDP Problem

The *key challenge* to solving the EDP problem is to structure our search over the space of all purification-augmented swapping trees to find the optimal one. The intermediate states in this search will be trees with optimal generation rates for a given pair of nodes (x, y) and fidelity f . To bound the set of intermediate states to explore, we consider only a finite set of discrete fidelity values $\mathcal{F} = \{f_1, f_2, \dots, f_n\}$. Thus, each tree considered will be for fidelity of at least f_i , for $i = 1..n$. With discrete fidelity values, $\lfloor f \rfloor$ means the largest $d_i \leq f$.

DP Algorithm. Let $T(x, y, f)$ be a tree with the least latency among all trees that generate EPs (x, y) with fidelity f or more, and let $L(x, y, f)$ be its latency. There are three cases:

- 1) The root of $T(x, y, f)$ is of the form $swap(x, y, z)$. Then the children of $T(x, y, f)$ are optimal for generating EP (x, z) and EP (z, y) with fidelities of at least f_1 and f_2 respectively, where $f = \lfloor F_{swap}(f_1, f_2) \rfloor$ (Eqn. 2).
- 2) The root of $T(x, y, f)$ is of the form $purify(x, y)$. Then the child is optimal for generating EP (x, y) with fidelity at least f_1 , where $f = \lfloor F_{pur}(f_1, f_1) \rfloor$ (Eqn. 5).

- 3) The root of $T(x, y, f)$ is of the form $link(x, y)$. Then (x, y) is a link in the network with fidelity f or more.

Thus, the problem has the *optimal substructure property*—the optimal solution to the problem uses optimal solutions to sub-problems—thereby enabling a dynamic programming solution. More formally, we can write the following recurrence for $L(x, y, f)$, the least latency as follows:

$$L(x, y, \lfloor f \rfloor) = \min\{l_s, l_p, l_l\} \quad (8)$$

where l_s , l_p , and l_l are the least latency among trees with *swap*, *purify*, and *leaf* at the root:

$$l_s = \min_z \left(L_{swap}(L(x, z, f_1), L(z, y, f_2)) \right) \quad (9)$$

where $f = F_{swap}(f_1, f_2)$

and L_{swap} and F_{swap} are as defined in Eqns. 1 and 2

$$l_p = \min_{i \in I} \{L_i(L(x, y, f_0), F_{pur,i}(f_0)) \mid F_{pur,i}(f_0) \geq f\} \quad (10)$$

where L_i is defined in Eqn. 7

$$l_l = \frac{1}{rate(x,y)} \text{ if } (x, y) \in E(Q) \text{ and } fid(x, y) \geq f \quad (11)$$

In the above, p_f and p_p denote the success rate of the swapping and purification operations, resp., and τ_c , τ_f , and τ_p are the latency for classical transmission, swapping operation, and purification operation, resp. We restrict each purification to have a bounded number of iterations (parameter I , Eqn. 10).

Optimality. It is easy to show that the above-described DP algorithm returns a purification-augmented swapping tree over (s, d) with fidelity f or higher with minimum expected generation latency among all purification-augmented swapping trees for given s, d , and f .

B. Optimal LP-based Solution to the GEDP Problem

In this section, we consider the GEDP problem and describe a solution based on linear programming to generate an optimal level-based structure (essentially, a *collection* of purification-augmented swapping trees, as described in §III-A) that maximizes the generation rate of EPs with fidelity exceeding the required threshold.

The Basic Idea. Given an instance of the GEDP problem, we create a hypergraph, with hypervertices representing EPs of certain fidelity between a pair of nodes, and hyperedges representing transformation between hypervertices. We then pose the optimization problem as a hypergraph flow problem and formulate it in terms of linear programming. As in the DP algorithm, we consider only a discrete set of fidelities \mathcal{F} .

Hypergraph. Given a GEDP problem over a quantum network Q and demand is Δ , we construct a hypergraph $H_{Q,\Delta}$ with hypervertices $V(H_{Q,\Delta})$ and edges $E(H_{Q,\Delta})$ as follows:

$V(H_{Q,\Delta})$ consists of:

- 1) Two distinguished vertices *start* and *term*
- 2) For each $u, v \in V(Q)$ and $f \in \mathcal{F}$, there are 4 hypervertices representing EPs (u, v) of fidelity at least f , produced using different operations:
 - a) *swap* (u, v, f) : EPs produced by an entanglement swap

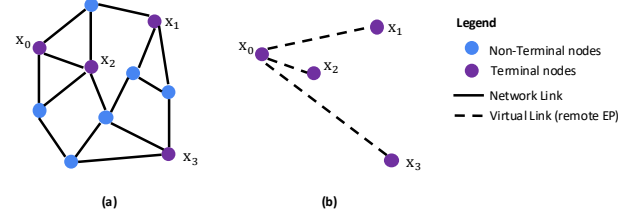


Fig. 4. The first stage of the distribution of GHZ states: the generation of virtual links between terminal nodes. (a) The quantum network and terminal nodes of the GHZ state. (b) The virtual links generated for the star-graph approach.

- b) *purify* $_1(u, v, f)$: EPs purified using two EPs of same fidelity
- c) *purify* $_2(u, v, f)$: EPs purified using two EPs of different fidelity
- d) *avail* (u, v, f) : a consolidation of EPs produced by different means

$E(H_{Q,\Delta})$ consists of:

- 1) [Start]: representing the generation of link EPs.
 - $(\{start\}, \{avail(u, v, fid(u, v))\}), \forall (u, v) \in E(Q)$
- 2) [Swap]: representing the entanglement swap operation.
 - $(\{avail(u, w, f_i), avail(w, v, f_j)\}, \{swap(u, v, f_k)\})$
 $\forall u, v, w \in V, f_i, f_j \in \mathcal{F}, f_k = \lfloor F_{swap}(f_i, f_j) \rfloor$
 - $(\{swap(u, v, f)\}, \{avail(u, v, f)\}), \forall u, v \in V, f \in \mathcal{F}$
- 3) [SelfPurify] representing purification using two copies of EPs with same fidelity.
 - $(\{avail(u, v, f)\}, \{purify_1(u, v, f')\})$
 $\forall u, v \in V(Q), f \in \mathcal{F}, f' = \lfloor F_{pur}(f, f) \rfloor$
 - $(\{purify_1(u, v, f)\}, \{avail(u, v, f)\}), \forall u, v \in V(Q)$
- 4) [PurifyDistinct] representing purification using two of EPs with different fidelity.
 - $(\{avail(u, v, f_i), avail(u, v, f_j)\}, \{purify_2(u, v, f_k)\})$
 $f_i, f_j \in \mathcal{F}, f_k = \lfloor F_{pur}(f_i, f_j) \rfloor$
 - $(\{purify_2(u, v, f)\}, \{avail(u, v, f)\}), \forall u, v \in V, f \in \mathcal{F}$
- 5) [Term] representing the generation of target EPs above the given fidelity threshold.
 - $(\{avail(s, d, f')\}, \{term\}), \forall (s, d, f) \in \Delta,$
 $f' \in \mathcal{F} \text{ s.t. } f' \geq f$

LP Variables, Constraints & Optimization Objective.

- *Variables*: z_e , for each hyperarc e in H , represents the EP generation rate at e 's tail.
- *Flow Constraints*, which vary with vertex types. Below, we use $out(v)$ and $in(v)$ to represent outgoing and incoming hyperedges from v .
 - For each vertex v s.t. $v = swap(\cdot)$:

$$\sum_{e \in in(v)} \frac{2}{3} z_e p_f \geq \sum_{e' \in out(v)} z_{e'}$$

This accounts for the loss due to the failure of the swap operation, and waiting for *both* EPs to arrive before the operation.

- For each vertex v s.t. $v = purify_1(\cdot)$:

$$\sum_{e \in in(v)} \frac{1}{2} z_e p_p \geq \sum_{e' \in out(v)} z_{e'}$$

The two EPs in self-purification have to be generated sequentially, hence the $\frac{1}{2}$ factor. The rate loss due to purification is factored in using p_p , the success probability of purification, which can be derived from fidelities of the vertices in the tails of the incoming hyperedges.

- For each vertex v s.t. $v = \text{purify}_2(\cdot)$:

$$\sum_{e \in \text{in}(v)} \frac{2}{3} z_e p_p \geq \sum_{e' \in \text{out}(v)} z_{e'}$$

Here, p_p models the rate loss due to purification, and the $\frac{2}{3}$ factor arises from waiting for *both* EPs to arrive before the operation.

- **Capacity Constraints:** For all hyperedges e from *start* to *avail*(u, v, f):
 $z_e \leq \text{rate}(u, v)$, where *rate* is specified by the quantum network graph Q .
- **Objective:** Maximize $\sum_{e \in \text{in}(\text{term})} z_e$

Optimality. It is straightforward to establish that the above-described LP formulation returns an optimal level-based structure over a set of source-destination pairs $\{(s_i, d_i)\}$ with minimum expected generation latency.

VI. Generating High-Fidelity GHZ States

There are two main challenges for extending our algorithms to GHZ states. First, an n -GHZ state can be constructed by fusing two smaller GHZ states (n_1 -GHZ and n_2 -GHZ states where $n = n_1 + n_2 - 1$), the number of intermediate states is exponential in the size of GHZ states. Second, an EP over nodes (x_i, x_j) can only be purified by copies of the same EP. In contrast, as explained below, an n -GHZ state can be purified by copies of itself [53] or by a *smaller-sized GHZ state*. This means that the construction may involve operations over intermediate structures that were built using common resources. Accounting for such shared resources leads to solutions with greater time complexity.

Purification of GHZ states. There are several existing methods for purifying GHZ states and graph states [20, 53–55]. Most assume that the target and sacrificial states are of the same size. They operate by comparing performing CNOT on corresponding qubits in the two states, measuring the sacrificial qubits, and succeeding if they are all identical. This can be readily extended to the case where the sacrificial state is a subset. Similar to EPs, we can define F_{fuse} and F_{GHZpur} to map the fidelity of operands of GHZ fusion and purification operations, respectively, to their results. Details are omitted.

A. Optimal DP Solution to the GDP Problem

We begin with a simplified strategy inspired by the fact that a GHZ state is locally equivalent to a star graph state. Then we propose three approximate strategies based on assumptions on the purification model, which greatly improves the time complexity without a significant effect on the efficiency.

For all these solutions, we use the following two-stage generation scheme [56]. In the first stage, we generate remote

EPs between the nodes in the GHZ state, treating this as an instance of the GEDP problem (§V). In the second stage, we perform fusion operations on these EPs to create the distributed GHZ states, treating the remote EPs generated in the first stage as virtual edges in a network.

Optimal DP Formulation: Assume after the generation of remote EPs in the first stage, we can view the network graph G as a star graph, $G = (V, E)$, $V = \{v_1, v_2, \dots, v_n\}$, $E = \{e_{12}, e_{13}, \dots, e_{1n}\}$, each edge has a certain EP generation rate k_e with the same fidelity f_e . The problem is to find k_e , the maximum generation rate of n -GHZ state over nodes (v_1, v_2, \dots, v_n) , over a fidelity threshold F_t . We assume that all the errors contribute equally to the fidelity of the GHZ state.

We define the DP algorithm as a recurrence over $T(S, k, \overrightarrow{EP})$, where T represents the maximum fidelity of GHZ state S that can be generated at rate k or higher, using a vector of elementary EPs over the underlying star graph. Note that unlike in §V, we formulate the recurrence in terms of *fidelity*, which means that the *rate* parameters will be drawn from a finite set of discrete values $\mathcal{K} = \{k_1, k_2, \dots\}$.

At each step in generating one n -GHZ state, we do one of the three operations:

- **Fusion(T_1, T_2):** Fusion of two GHZ states:

$$\begin{aligned} T(S_1 \cup S_2, \lfloor \frac{2}{3} p_f k \rfloor, \overrightarrow{EP}_1 + \overrightarrow{EP}_2) \\ = F_{\text{fuse}}(T(S_1, k, \overrightarrow{EP}_1), T(S_2, k, \overrightarrow{EP}_2)) \end{aligned}$$

- **Self_purification(T_1):** Purification sacrificing an n -GHZ:

$$T(S, \lfloor \frac{1}{2} p_p k \rfloor, \overrightarrow{EP}) = F_{\text{GHZpur}}(T(S, k, \overrightarrow{EP}))$$

- **Subset_purification(T_1, T_2):** Purification sacrificing a n' -GHZ with a subset, with $S_1 \subset S_2$:

$$\begin{aligned} T(S_1, \lfloor \frac{2}{3} p_p k \rfloor, \overrightarrow{EP}_1 + \overrightarrow{EP}_2) \\ = F_{\text{GHZpur}}(T(S_1, k, \overrightarrow{EP}_1), T(S_2, k, \overrightarrow{EP}_2)) \end{aligned}$$

The base case arises when S is an EP, $k \in \mathcal{K}$, and \overrightarrow{EP} a vector with k at S and 0 elsewhere. Then $T(S, k, \overrightarrow{EP}) = f_e$.

In the above, p_f is the success probability of fusion, and p_p is the success rate of the purification operation.

Approximate DP Formulations: Since we have to keep track of the shared resources, the time complexity of the optimal DP formulation above is $O(4^{|\mathcal{K}|})^n$, where n is the size of the goal GHZ state. Note that the exponent n is not the size of the network. The $|\mathcal{K}|^n$ factor may be prohibitive, and we introduce three approximations that abstract resource usage by maintaining a single number instead of \overrightarrow{EP} . This reduces the time complexity to $O(4^n)$.

- 1) **Same size purification (SS):** Considers only fusion and same-size purification operations.
- 2) **One-time purification (OT):** As in SS, consider a single subset-purification between fusion operations. This considers a larger solution space than SS, but has the same time complexity.
- 3) **EP-based purification (2G):** Considers only fusion and subset-purification where the subset is a 2-GHZ (EP).

B. Optimal LP-Based Solution to the GGDP Problem

Similar to the case of EPs in § V-B, we can build an LP-based optimization framework for constructing an optimal level-based fusion structure for generating a collection of GHZ states exceeding given fidelity thresholds. We can construct a similar hypergraph whose optimal flow represents an optimal level-based structure. The non-trivial vertices of the hypergraph are of the form $avail(S, f)$, $fuse(S, f)$, $purify_1(S, f)$ and $purify_2(S, f)$ where S represent a subset of the goal GHZ state, and f is a discretized fidelity $\in \mathcal{F}$. Edges of the hypergraph correspond to fusion and purification operations. There are $O(2^n |\mathcal{F}|)$ hypervertices, and $O(4^n |\mathcal{F}|^2)$ hyperedges. Solving the flow problem entails attaching a variable to each hyperedge, constraining the flow at each node, and representing capacity constraints.

VII. Evaluations

We evaluated the optimal solutions generated by our algorithms and the protocols from existing works using the quantum network simulator NetSquid [57].

Netsquid Protocol. We build our protocols on top of the link-layer protocol of [58], delegated to continuously generate EPs on a link at a desired rate. The key aspect of our protocols is that a swapping or a fusion operation is done only when *both* appropriate EPs or GHZ states have been generated, and a purification operation is done only when *both* appropriate target and sacrificial states are generated. Swapping/fusion/purification operations were implemented to transmit classical information to all relevant nodes upon success. On failure, the qubits of the entanglement state are discarded, allowing the protocols to generate new link EPs from scratch. During the purification process, the sacrificial state is consumed through measurements.

Simulation Setting. We generate random quantum networks in a similar way as in the recent works [23, 34, 56]. By default, we use a network spread over an area of $100km \times 100km$. We use the Waxman model [59], used to create Internet topologies, distribute the nodes, and create links. We vary the number of nodes from 30 to 70 (the default is 50) and the edge density from 0.05 to 0.2 with a default value of 0.1. For the distribution of high-fidelity GHZ states, we vary the size of GHZ states from 4 to 10 qubits (the default is 6), each qubit on different terminal nodes. For each remote EP, we set the generation rate to range from 10/s to 90/s (with a default of 50/s), as determined by the first stage and used as the initial value for the second stage. For EP generation, the fidelity of each link EP is a random number between 0.7 and 0.95, the fidelity threshold for goal EP state is 0.8, the same as the most similar work [36]. For GHZ generation, the fidelity of each link EP is set to 0.9, and the fidelity threshold for the goal GHZ state is 0.9. Each data point is for a 100-second simulation in NetSquid for EP and GHZ generation.

Parameter Values. We use parameter values similar to the ones used in [23, 28]. In particular, we use swapping/fusion probability of success (p_f) to be 0.4 and latency (τ_f) to be 10 μ secs;

in some plots, we vary p_f from 0.2 to 0.6. The atomic-BSM probability of success (p_b) and latency (τ_b) always equal their fusion counterparts p_f and τ_f . The optical-BSM probability of success (p_{ob}) is half of p_b . For generating link-level EPs, we use atom-photon generation times (τ_g) and probability of success (p_g) as 50 μ sec and 0.33, respectively. Finally, we use photon transmission success probability as $e^{-d/(2L)}$ [28] where L is the channel attenuation length (chosen as 20km for optical fiber) and d is the distance between the nodes. In NetSquid, we pick the depolarizing channel as our noise model and set the depolarization rate as 0.01.

Prior Algorithms Compared. For comparison with prior work, we implement two schemes for EP: a recent end-to-end-fidelity-based scheme based on [36] (called E2E) and a naive approach (called LP-Naive), and one naive scheme for GHZ state (also called LP-Naive). E2E has three steps: First, find the top ten shortest (fidelity-based weights) paths for each pair of source and destination nodes; then, for each path, purify all the links above a link fidelity threshold to guarantee that the end-to-end is above the fidelity threshold, using the right-deep swapping trees; finally, using linear programming to allocate limited resources among different paths, maximizing the generation rate. The LP-Naive scheme uses LP-based methods to generate EPs or GHZ states, restricting purification to the top level only. In LP-Naive, only the desired EPs or GHZ states can serve as sacrificial states.

Our Algorithms. For the generation of EPs, we implement the LP and DP schemes. To compare the results for multiple source-destination pairs, we use a modified DP scheme (called DP-Iterative), which first employs the original DP method to identify a purification-augmented swapping tree. It then removes the resources utilized by this tree and iteratively applies the DP scheme to identify additional purification-augmented swapping trees. For the generation of GHZ states, we implement the LP scheme and the three DP-based approximate schemes, DP-ss, DP-OT, and DP-2G.

Evaluation Results. Figs.5-6 show the generation rates of various schemes for EPs and GHZ states, as determined by the NetSquid simulations of at least 100-second duration. In particular, we vary one parameter at a time while keeping the other parameters constant (to their default values). For the generation of EPs, we observe that our LP scheme outperforms the LP-Naive and E2E schemes nearly by a factor of three in most cases. And, our DP scheme consistently outperforms the LP-Naive and E2E schemes, even in cases where our DP scheme only finds one purification-augmented swapping tree while the LP-Naive and E2E schemes find multiple trees.

Fig. 7 shows the results for multiple source-destination pairs, the generation rate of the LP-Naive and E2E schemes are similar, and our DP scheme outperforms these two schemes by more than 50%, our LP scheme outperforms these two schemes by more than 100%. Fig. 8 shows the results varying the fidelity for link EPs for 7 pairs of sources and destinations. Our LP scheme still outperforms other schemes, and the performance of LP-Naive is highly influenced by link fidelity,

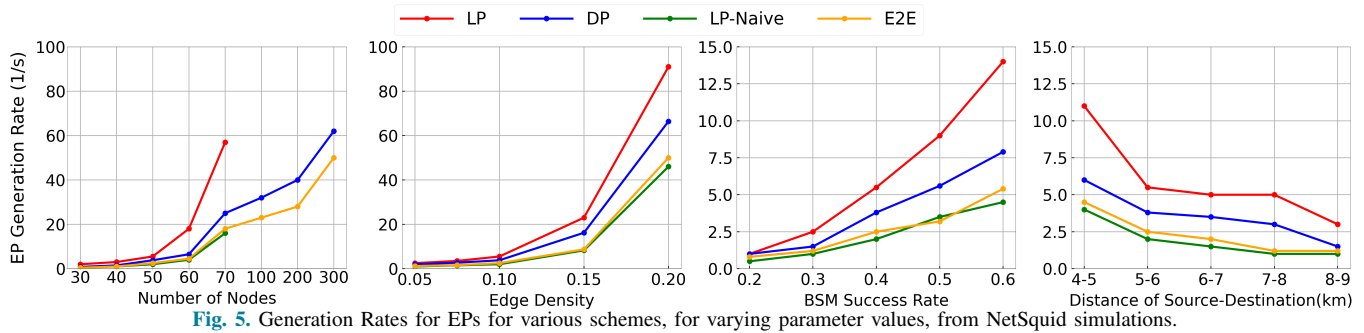


Fig. 5. Generation Rates for EPs for various schemes, for varying parameter values, from NetSquid simulations.

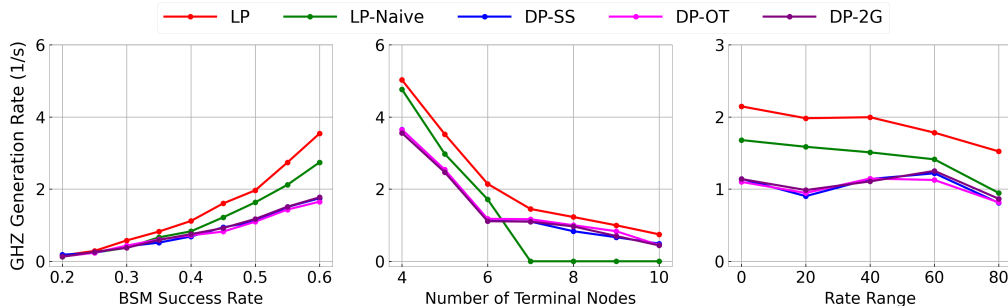


Fig. 6. Generation Rates for GHZ states for various schemes, for varying parameter values, from NetSquid simulations.

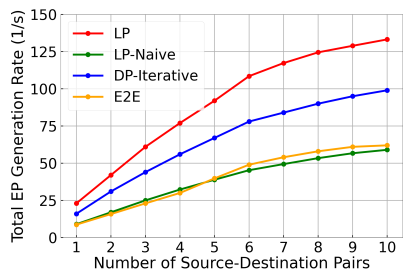


Fig. 7. EP generation rates for a varying number of source-destination pairs (the edge density is 0.2, larger than the default, ensuring we can find purification-augmented swapping trees between all sources and destinations).

and it performs poorly when link fidelity is low.

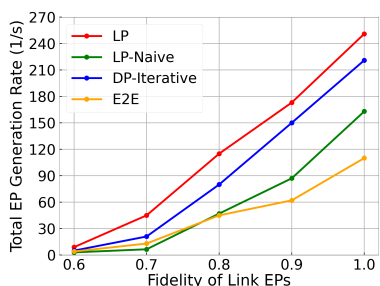


Fig. 8. EP generation rates for varying the fidelity of link EPs.

For the generation of GHZ states, we observe that our LP scheme outperforms the LP-Naive scheme while our DP-SS, DP-OT, and DP-2G result in a lower generation rate. As the number of terminal nodes increases, the rate of the LP-Naive scheme suddenly drops to zero, for the following reason. When the GHZ state is sufficiently large, we reach the top level after several fusions, but by this point, the fidelity is so low that no purification can improve it. As a result, the fidelity cannot exceed the required threshold, and

the generation rate will be zero.

Scalability of the algorithms. We ran DP and LP-based algorithms on an AMD Ryzen 9 7950X3D CPU machine. We observed that our DP-based scheme takes about 1 minute for EPs to run for a 100-node network with low memory use. This represents an acceptable performance for practical use. The LP-based scheme can take several minutes to hours and requires substantial memory on large networks. For GHZ states, our DP-SS scheme takes about 4 minutes to run, with low memory use, for a GHZ state of 7 terminal nodes. Our LP-based scheme requires less time than our DP-based schemes, but its memory usage increases rapidly. These schemes will require further optimization and/or parallelization when applied to GHZ states with many terminal nodes.

VIII. CONCLUSIONS

We considered the problems of maximizing the generation rate of distributed EPs and GHZ states that exceed a given fidelity threshold. Evaluations show that our algorithms provide better solutions than existing protocols, and our algorithms are feasible in practice. Our techniques can be readily generalized to a “quantity model” such as [44] that considers the counts of EPs instead of their rates. Our future work is focused on incorporating the effect of time-dependent decoherence and on the distribution of general graph states.

REFERENCES

- [1] C. Simon, “Towards a global quantum network,” *Nature Photonics*, vol. 11, no. 11, pp. 678–680, 2017.
- [2] V. Scarani *et al.*, “The security of practical quantum key distribution,” *Reviews of modern physics*, 2009.
- [3] C. H. Bennett and G. Brassard, “Quantum cryptography: Public key distribution and coin tossing,” *Theoretical computer science*, vol. 560, pp. 7–11, 2014.
- [4] S. Pirandola *et al.*, “Advances in quantum cryptography,” *Advances in Optics and Photonics*, 2020.

- [5] V. Scarani, H. Bechmann-Pasquinucci, N. J. Cerf, M. Dušek, N. Lütkenhaus, and M. Peev, “The security of practical quantum key distribution,” *Reviews of modern physics*, vol. 81, no. 3, pp. 1301–1350, 2009.
- [6] C. Zhan, H. Gupta, and M. Hillery, “Optimizing initial state of detector sensor networks,” *ACM Transactions on Quantum Computing*, vol. 5, no. 2, pp. 1–25, 2024.
- [7] Z. Eldredge, M. Foss-Feig, J. A. Gross, S. L. Rolston, and A. V. Gorshkov, “Optimal and secure measurement protocols for quantum sensor networks,” *Physical Review A*, vol. 97, no. 4, p. 042337, 2018.
- [8] C. Zhan and H. Gupta, “Quantum sensor network algorithms for transmitter localization,” in *2023 IEEE International Conference on Quantum Computing and Engineering (QCE)*, vol. 1. IEEE, 2023, pp. 659–669.
- [9] M. Hillery, H. Gupta, and C. Zhan, “Discrete outcome quantum sensor networks,” *Physical Review A*, vol. 107, no. 1, p. 012435, 2023.
- [10] R. G. Sundaram and H. Gupta, “Dynamic distribution of quantum circuits with minimum execution time,” in *2025 International Conference on Quantum Communications, Networking, and Computing (QNCN)*. IEEE, 2025.
- [11] M. Caleffi, M. Amoretti, D. Ferrari, J. Illiano, A. Manzalini, and A. S. Cacciapuoti, “Distributed quantum computing: a survey,” *Computer Networks*, vol. 254, p. 110672, 2024.
- [12] R. G. Sundaram, H. Gupta, and C. Ramakrishnan, “Distributing quantum circuits with minimum circuit execution time over quantum networks,” in *2024 IEEE International Conference on Quantum Computing and Engineering (QCE)*, vol. 1. IEEE, 2024, pp. 1938–1948.
- [13] J. I. Cirac, A. Ekert, S. F. Huelga, and C. Macchiavello, “Distributed quantum computation over noisy channels,” *Physical Review A*, vol. 59, no. 6, p. 4249, 1999.
- [14] R. G. Sundaram and H. Gupta, “Distributing quantum circuits using teleportations,” in *2023 IEEE International Conference on Quantum Software (QSW)*. IEEE, 2023, pp. 186–192.
- [15] R. G. Sundaram, H. Gupta, and C. Ramakrishnan, “Distribution of quantum circuits over general quantum networks,” in *2022 IEEE International Conference on Quantum Computing and Engineering (QCE)*. IEEE, 2022, pp. 415–425.
- [16] R. G. Sundaram, H. Gupta, and C. Ramakrishnan, “Efficient distribution of quantum circuits,” in *35th International Symposium on Distributed Computing (DISC 2021)*. Schloss Dagstuhl-Leibniz-Zentrum für Informatik, 2021.
- [17] D. Main, P. Drmota, D. Nadlinger, E. Ainley, A. Agrawal, B. Nichol, R. Srinivas, G. Araneda, and D. Lucas, “Distributed quantum computing across an optical network link,” *Nature*, pp. 1–6, 2025.
- [18] H.-J. Briegel, W. Dür, J. I. Cirac, and P. Zoller, “Quantum repeaters: the role of imperfect local operations in quantum communication,” *Physical Review Letters*, vol. 81, no. 26, p. 5932, 1998.
- [19] C. H. Bennett *et al.*, “Purification of noisy entanglement and faithful teleportation via noisy channels,” *Physical Review Letters*, 1996.
- [20] W. Dür *et al.*, “Entanglement purification and quantum error correction,” *Reports on Progress in Physics*, vol. 70, no. 8, p. 1381, 2007.
- [21] G. Zhao, J. Wang, Y. Zhao, H. Xu, L. Huang, and C. Qiao, “Segmented entanglement establishment with all-optical switching in quantum networks,” *IEEE/ACM Transactions on Networking*, vol. 32, no. 1, pp. 268–282, 2023.
- [22] L.-M. Duan, M. D. Lukin, J. I. Cirac, and P. Zoller, “Long-distance quantum communication with atomic ensembles and linear optics,” *Nature*, vol. 414, no. 6862, pp. 413–418, 2001.
- [23] M. Ghaderibaneh *et al.*, “Efficient quantum network communication using optimized entanglement swapping trees,” *IEEE TQE*, 2022.
- [24] S. de Bone *et al.*, “Protocols for creating and distilling multipartite ghz states with bell pairs,” *IEEE Transactions on Quantum Engineering*, vol. 1, pp. 1–10, 2020.
- [25] M. Ghaderibaneh, H. Gupta, and C. Ramakrishnan, “Generation and distribution of ghz states in quantum networks,” in *2023 IEEE International Conference on Quantum Computing and Engineering (QCE)*, vol. 1. IEEE, 2023, pp. 1120–1131.
- [26] A. Manzalini, “Quantum communications in future networks and services,” *Quantum Reports*, vol. 2, no. 1, pp. 221–232, 2020.
- [27] F. Mazza, C. Zhan, J. Chung, R. Kettimuthu, M. Caleffi, and A. S. Cacciapuoti, “Simulation of entanglement-enabled connectivity in qns using sequence,” *arXiv preprint arXiv:2411.11031*, 2024.
- [28] M. Caleffi, “Optimal routing for quantum networks,” *IEEE Access*, 2017.
- [29] M. A. Nielsen and I. L. Chuang, *Quantum computation and quantum information*. Cambridge university press Cambridge, 2001, vol. 2.
- [30] C. H. Bennett *et al.*, “Mixed-state entanglement and quantum error correction,” *Physical Review A*, 1996.
- [31] W. Dür *et al.*, “Quantum repeaters based on entanglement purification,” *Physical Review A*, vol. 59, no. 1, p. 169, 1999.
- [32] H. Gu *et al.*, “Fendi: Toward high-fidelity entanglement distribution in the quantum internet,” *IEEE/ACM Transactions on Networking*, 2024.
- [33] D. Deutsch *et al.*, “Quantum privacy amplification and the security of quantum cryptography over noisy channels,” *Physical review letters*, vol. 77, no. 13, p. 2818, 1996.
- [34] S. Shi and C. Qian, “Concurrent entanglement routing for quantum networks: Model and designs,” in *SIGCOMM*, 2020.
- [35] R. G. Sundaram and H. Gupta, “Optimized generation of entanglement by real-time ordering of swapping operations,” *arXiv preprint arXiv:2405.07501*, 2024.
- [36] Y. Zhao *et al.*, “E2e fidelity aware routing and purification for throughput maximization in quantum networks,” in *IEEE INFOCOM*, 2022.
- [37] V. Kumar *et al.*, “Routing in quantum repeater networks with mixed noise figures,” *arXiv preprint arXiv:2310.08990*, 2023.
- [38] G. Iacovelli *et al.*, “A probability-based optimization approach for entanglement distribution and source position in quantum networks,” *IEEE Journal on Selected Areas in Communications*, 2024.
- [39] C. Li *et al.*, “Effective routing design for remote entanglement generation on quantum networks,” *npj Quantum Information*, 2021.
- [40] N. K. Panigrahy *et al.*, “On the capacity region of a quantum switch with entanglement purification,” in *IEEE INFOCOM*, 2023.
- [41] S. Pouryousef *et al.*, “A quantum overlay network for efficient entanglement distribution,” in *IEEE INFOCOM 2023*, 2023, pp. 1–10.
- [42] C. Zhan, J. Chung, A. Zang, A. Kolar, and R. Kettimuthu, “Design and simulation of the adaptive continuous entanglement generation protocol,” *arXiv preprint arXiv:2502.01964*, 2025.
- [43] M. Victora *et al.*, “Entanglement purification on quantum networks,” *Physical Review Research*, vol. 5, no. 3, p. 033171, 2023.
- [44] S. Santos *et al.*, “Shortest path finding in quantum networks with quasi-linear complexity,” *IEEE Access*, vol. 11, pp. 7180–7194, 2023.
- [45] Z. Jia and L. Chen, “From entanglement purification scheduling to fidelity-constrained multi-flow routing,” *arXiv preprint arXiv:2408.08243*, 2024.
- [46] L. Chen and Z. Jia, “On optimum entanglement purification scheduling in quantum networks,” *IEEE Journal on Selected Areas in Communications*, 2024.
- [47] J. Wallnöfer *et al.*, “Multipartite state generation in quantum networks with optimal scaling,” *Scientific reports*, vol. 9, no. 1, p. 314, 2019.
- [48] A. Kay *et al.*, “Multipartite purification protocols: Upper and optimal bounds,” *Physical Review A*, vol. 75, no. 6, p. 062307, 2007.
- [49] H. Qin *et al.*, “Efficient multipartite entanglement purification with non-identical states,” *arXiv preprint arXiv:2311.10250*, 2023.
- [50] T. Carle *et al.*, “Purification to locally maximally entangleable states,” *Physical Review A*, vol. 87, no. 1, p. 012328, 2013.
- [51] N. H. Nickerson *et al.*, “Topological quantum computing with a very noisy network and local error rates approaching one percent,” *Nature communications*, vol. 4, no. 1, p. 1756, 2013.
- [52] S. de Bone *et al.*, “Protocols for creating and distilling multipartite ghz states with bell pairs,” *IEEE Transactions on Quantum Engineering*, vol. 1, pp. 1–10, 2020.
- [53] E. N. Maneva and J. A. Smolin, “Improved two-party and multi-party purification protocols,” *Contemporary Mathematics*, vol. 305, pp. 203–212, 2002.
- [54] M. Murao *et al.*, “Multipartite entanglement purification protocols,” *Physical Review A*, vol. 57, no. 6, p. R4075, 1998.
- [55] W. Dür *et al.*, “Multipartite entanglement purification for graph states,” *Physical review letters*, vol. 91, no. 10, p. 107903, 2003.
- [56] X. Fan *et al.*, “Optimized distribution of entanglement graph states in quantum networks,” *arXiv preprint arXiv:2405.00222*, 2024.
- [57] T. Coopmans *et al.*, “NetSquid, a discrete-event simulation platform for quantum networks,” *Communications Physics*, 2021.
- [58] A. Dahlberg *et al.*, “A link layer protocol for quantum networks,” in *SIGCOMM*, 2019.
- [59] B. Waxman, “Routing of multipoint connections,” *IEEE Journal on Selected Areas in Communications*, 1988.